Supporting Information

Impact of Photo-Induced Degradation of Electron Acceptors on Photophysics, Charge Transport and Device Performance of All-Polymer and Fullerene-Polymer Solar Cells

Taesu Kim,[1] Robert Younts,[2] Wonho Lee,[1] Seungjin Lee,[1] Kenan Gundogdu[*, 2] and Bumjoon J. Kim*[*,1]*

[1] Department of Chemical and Biomolecular Engineering, Korea Advanced Institute of Science and Technology (KAIST), Daejeon 34141, Korea

[2] Department of Physics, North Carolina State University, Raleigh, North Carolina 27695, United States

*Email - bumjoonkim@kaist.ac.kr, bjmanse2@gmail.com

Table of Contents

References

Methods

SCLC measurement: The hole and electron mobilities of the all-polymer blends were measured by the SCLC method using ITO/PEDOT:PSS/polymer blends/Au and ITO/ZnO/polymer blends/LiF/Al devices, respectively. Current-voltage measurements in the range of 0-8 V were taken, and the results were fitted to a space-charge-limited function. The SCLC is described by:

$$J_{SCLC} = \frac{9}{8}\varepsilon\varepsilon_0\mu\frac{V^2}{L^3} \quad (1)$$

where ε_0 is the permittivity of free space (8.85×10^{-14} F cm^{-1}), ε is the relative dielectric constant of the active layer (3.2 for PBDTTTPD and P(NDI2HD-T) and 3.9 for fullerene), μ is the mobility of the charge carriers, V is the potential across the device ($V = V_{applied}-V_{bi}-V_r$), and L is the active layer thickness. The series and contact resistances of the device (15-25 Ω) were measured using blank devices (ITO/PEDOT:PSS/Au and ITO/ZnO/LiF/Al, respectively), and the voltage drop caused by this resistance (V_r) was subtracted from the applied voltage.

Multivariate Curve Resolution with Alternating Least Squares (MCR-ALS): The purpose of the analysis is to used soft-modeling (physical constaints) to find the best possible component spectra for excited-state species to described the TA surface and derive the resulting kinetics for each species. This analysis is detailed in the previous papaer[1] and utilized in the following papers[2, 3] The TA surface for p excited-state species is described by $D = CS + E$, where D is a m by n TA data matrix, C is a p x n concentration profile (kinetics) matrix, and S is the m by p spectral profile matrix, and E is the error matrix. Initial S matrix is built from a guess of spectral profiles, specifically the singlet exciton absorption profile for the neat PBDTTTPD film. Then

using least squares the concentration profiles are calculated and constraints of non-negativity are applied. Then the spectral profiles are solved for using least squares and constaints of non-negativity, unimodality, and fixed known singlet exciton spectra are applied. Then a mean-squared error (MSE) is determined. If the MSE is within tolerance then the alternating least squares (ALS) process halts and the spectra and kinectic components are determined. If the MSE is not within the tolerance, then the ALS process is repeated until the MSE converges or reaches the specified tolerance. To improve analysis results, multiple normalized TA surfaces can be concatenated to form an augmented matrix described by the same p spectral profiles, which in our case of SE and CS profiles. We created an augmented matrix from the four measurements of the 0, 6, 12, and 24 hour exposure samples and the other three measurements from the fluence dependent measurements on the 0 hour sample.

Polaron Generation Modeling: To determine if formation times of polarons in all-PSC for different solar illumination times, we fit the first 100 ps to a bi-exponential function

$$N_{CS}(t) = A_1\left(1 - e^{-\frac{t}{\tau_1}}\right) + A_2\left(1 - e^{-\frac{t}{\tau_2}}\right) \quad (2)$$

where A_1 and A_2 are represent the proportions of sub-picosecond, τ_1, and picosecond, τ_2, charge generation, respectively. Similarities in the polaron formation analysis for varied solar illumination in Table S2 show no indication of change with solar illumination.

Supplementary Figures

Table S1. Photovoltaic Characteristics for PBDTTTPD:PCBM and PBDTTTPD:P(NDI2HD-T) devices.

Electron acceptors	**ABL**	V_{OC} **(V)**	J_{SC} **(mA cm^{-2})**	***FF***	**PCE[a] (%)**
PCBM	MoO_3	0.96	10.13	0.54	5.24
P(NDI2HD-T)	MoO_3	1.03	10.77	0.59	6.55
PCBM	PEDOT:PSS	0.90	8.40	0.50	3.81
P(NDI2HD-T)	PEDOT:PSS	1.00	9.30	0.51	4.75

[a] Photovoltaic characteristics obtained under AM 1.5 G-simulated solar illumination (100 mW cm^{-2}).

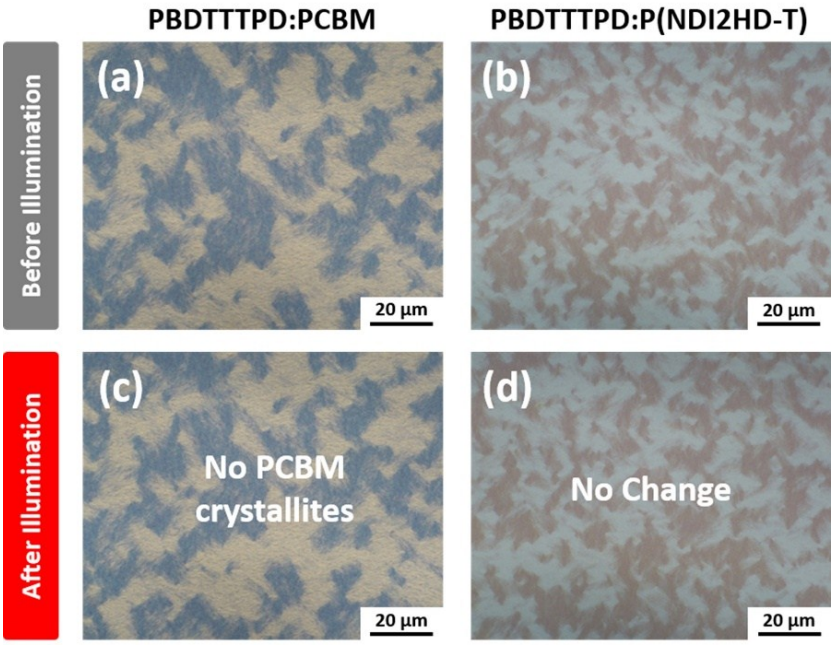

Figure S1. Optical microscope images showing morphology changes in the optimized active layer of PBDTTTPD:PCBM and PBDTTTPD:P(NDI2HD-T) blend films before (**a** and **b**) and after (**c** and **d**) 12 h illumination under one sunlight, respectively. No morphological changes were observed for both films after illumination.

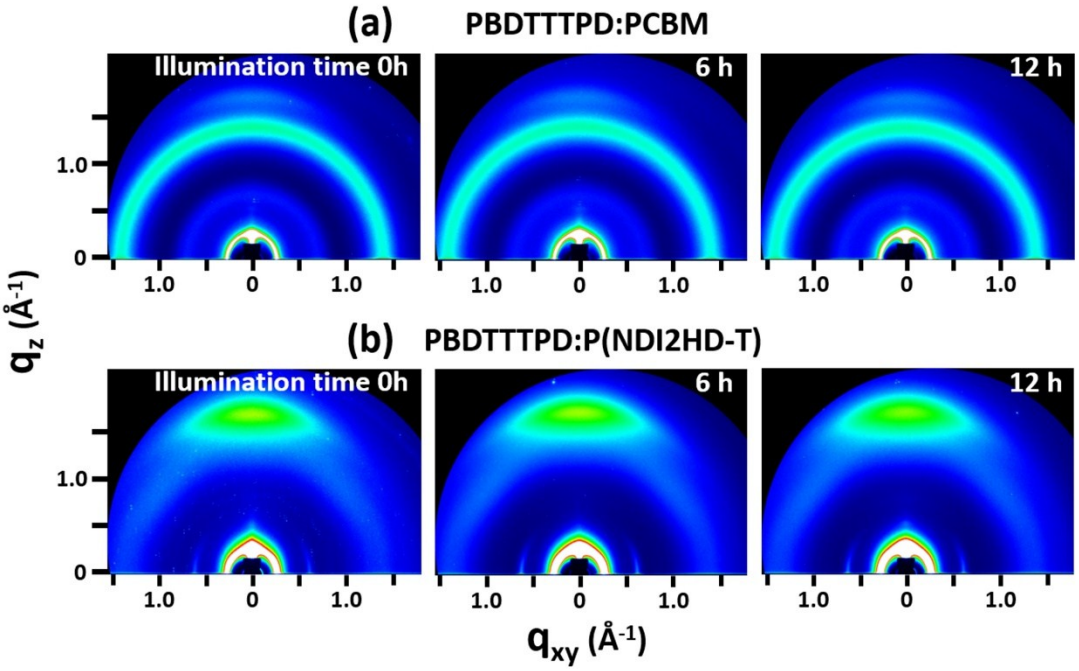

Figure S2. 2D GIXS images of (**a**) PCBM-PSCs and (**b**) all-PSCs blends under one sunlight illumination for different times.

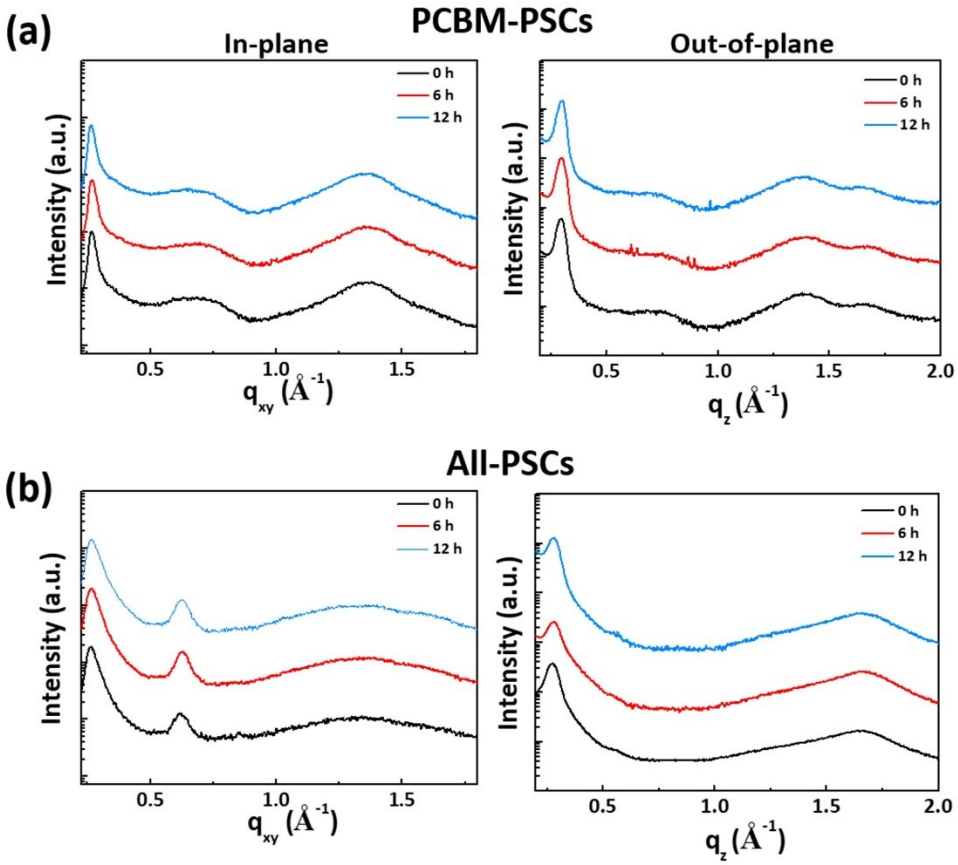

Figure S3. GIXS linecuts in the in-plane and out-of-plane directions for (**a**) PBDTTTPD:PCBM and (**b**) PBDTTTPD:P(NDI2HD-T) blend films under one sunlight illumination for different times.

Before illumination, the BHJ blend of the PBDTTTPD:PCBM exhibited prominent a (010) peak at $q_z \approx 1.7$ Å^{-1} in the out-of-plane direction, corresponding to the π–π stacking of PBDTTTPD, indicating the preferential face-on orientation of the donor polymer relative to the substrate. In addition, diffuse halos ($q \approx 0.7$ and $q \approx 1.4$ Å^{-1}) from amorphous PCBM molecules were observed. In the case of all-PSC, both the PBDTTTPD and P(NDI2HD-T) exhibited a prominent (010) π–π stacking peaks in the out-of-plane direction, while the (100) lamellar peaks ($q_{xy} \approx 0.27$ Å^{-1}) of the PBDTTTPD and P(NDI2HD-T) and the (001) peak ($q_{xy} \approx 0.6$ Å^{-1}) of the P(NDI2HD-T) polymer were observed in the in-plane direction, suggesting that the two polymers are preferentially orientated to face-on directions.[4] After illumination, in both PSC systems, the locations and intensities of the scattering peaks were not altered, indicating their polymer packing structures and the face-on geometry were well preserved. Therefore, the photo-degradation in the device performance of the PBDTTTPD:PCBM is not associated with the morphological and structural changes of the active layer.

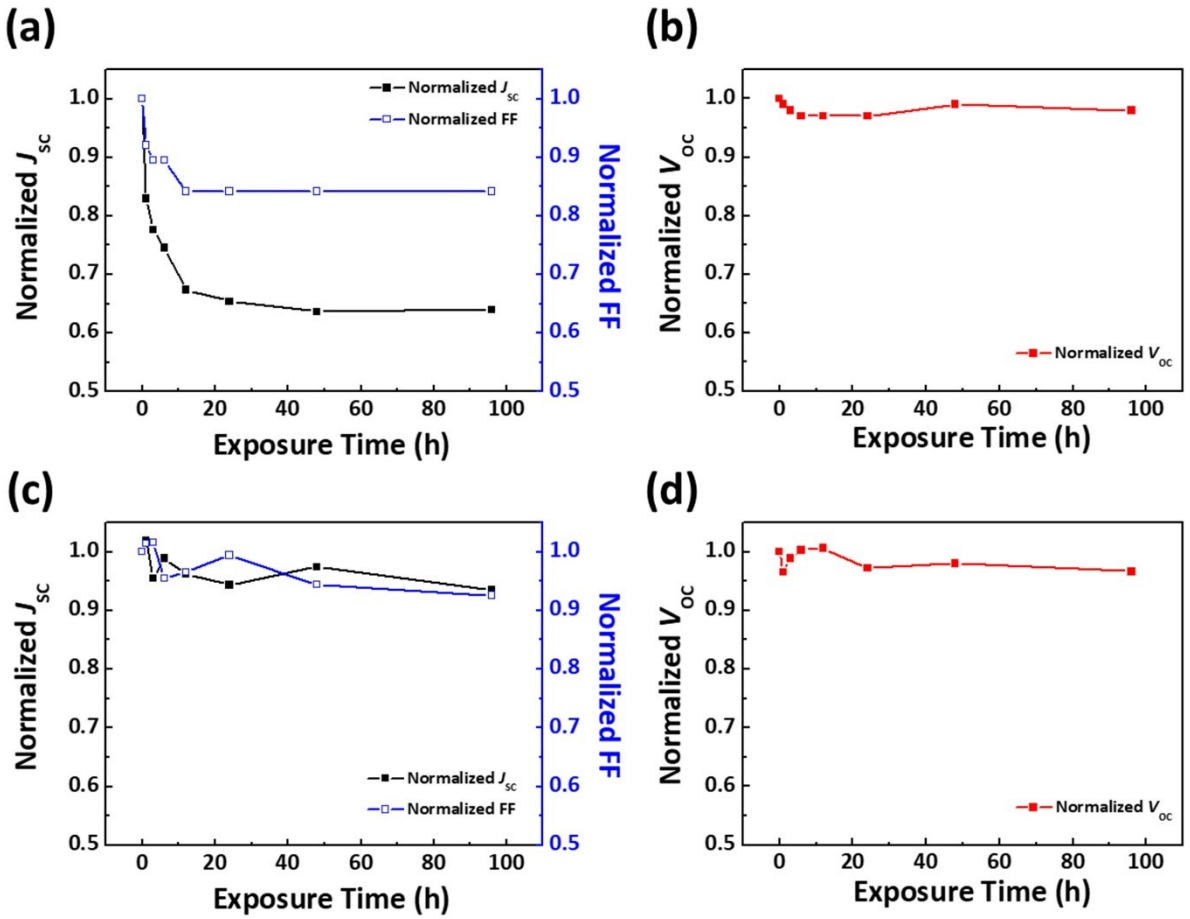

Figure S4. Normalized J_{SC} and FF of (**a**) PCBM-PSCs and (**c**) all-PSCs and normalized V_{OC} of (**b**) PCBM-PSCs and (**d**) all-PSCs as function of illumination times.

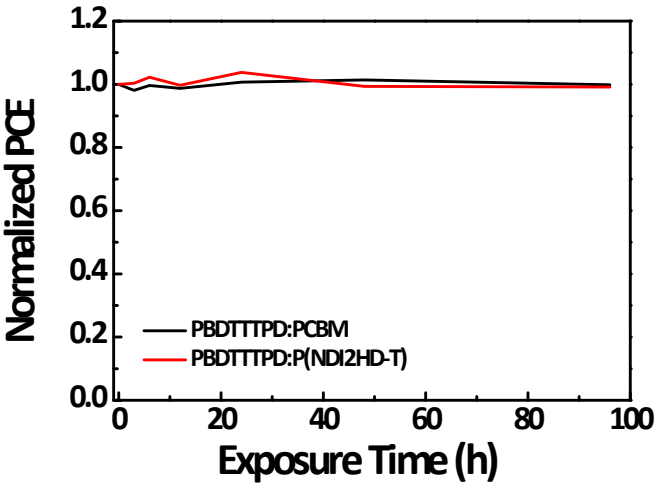

Figure S5. Normalized efficiencies of PCBM- and all-PSCs measured in dark condition.

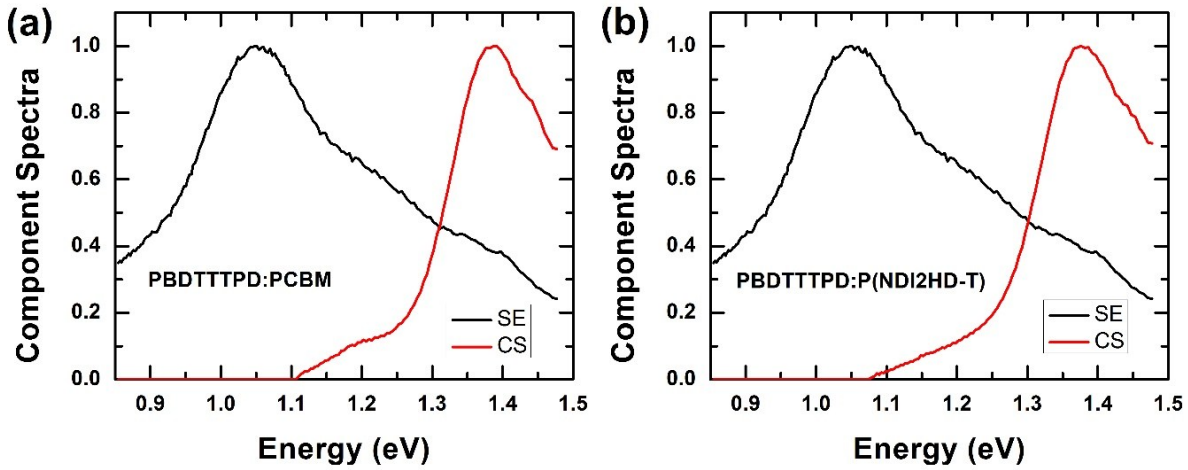

Figure S6. TA component spectra from MCR-ALS analysis for (**a**) PBDTTTPD:PCBM and (**b**) PBDTTTPD:PNDI2HDT films.

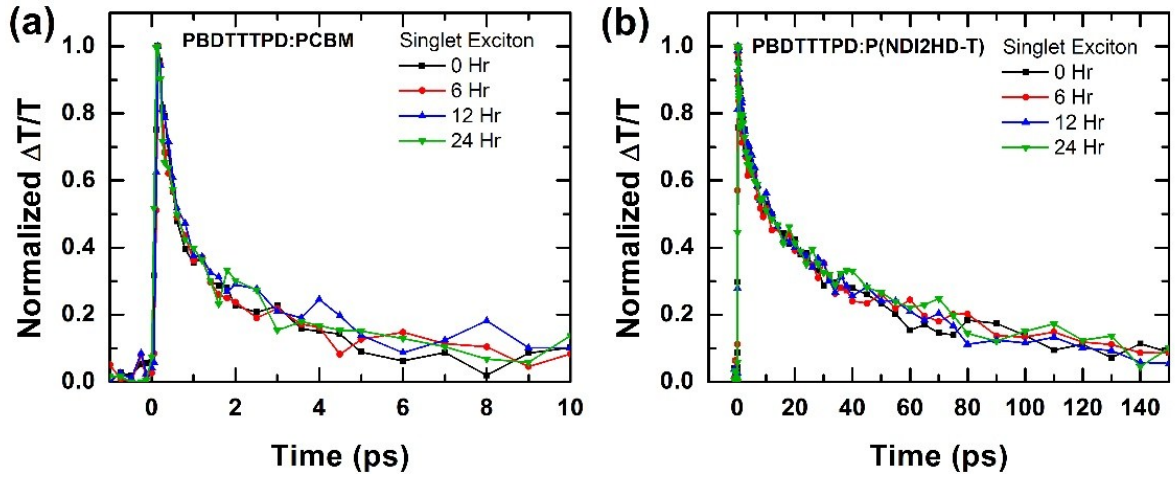

Figure S7. TA dynamics of the singlet exciton absorption peak for (**a**) PBDTTTPD:PCBM film and (**b**) PBDTTTPD:PNDI2HDT film under one sunlight illumination for different times.

Table S2. Polaron formation kinetics for PBDTTTPD:P(NDI2HD-T) for varying solar illumination time. Note that parameter error is shown for time constants in parenthesis.

Illumination Time (h)	A_1	τ_1	A_2	τ_2
0	44%	0.87 (0.2) ps	56%	18 (3) ps
6	44%	0.44 (0.1) ps	56%	14 (2) ps
12	45%	0.43 (0.1) ps	55%	13 (2) ps
24	36%	0.79 (0.3) ps	64%	11 (3) ps

Table S3. Fit parameters for CS dynamics for PBDTTTPD:PCBM and PBDTTTPD:P(NDI2HD-T) films with different illumination times.

Fit Parameter	System	0 h	6 h	12 h	24 h
A (%)	PCBM-PSC	64 ± 2	56 ± 2	56 ± 3	52 ± 2
	All-PSC	34 ± 2	34 ± 2	33 ± 2	29 ± 4
τ (ns)	PCBM-PSC	1.1 ± 0.1	1.7 ± 0.2	1.8 ± 0.2	1.2 ± 0.1
	All-PSC	2.0 ± 0.4	1.5 ± 0.3	1.5 ± 0.3	2.4 ± 0.9
B (%)	PCBM-PSC	36 ± 2	44 ± 2	44 ± 3	48 ± 2
	All-PSC	66 ± 2	66 ± 2	67 ± 2	71 ± 4

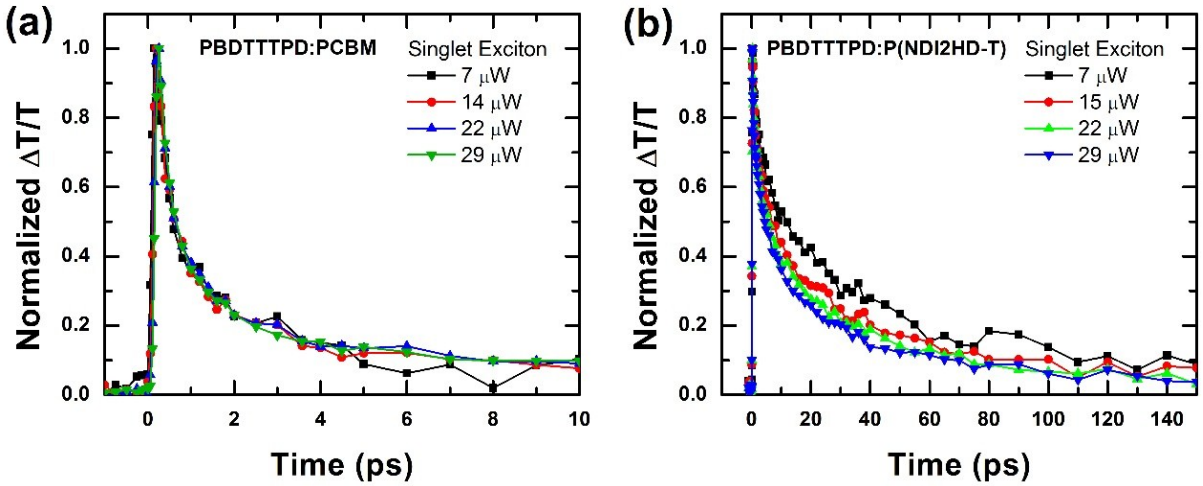

Figure S8. Fluence dependent dynamics of the SE peak before irradiation of the (a) PBDTTTPD:PCBM blended film and (b) PBDTTTPD:P(NDI2HD-T) blended film.

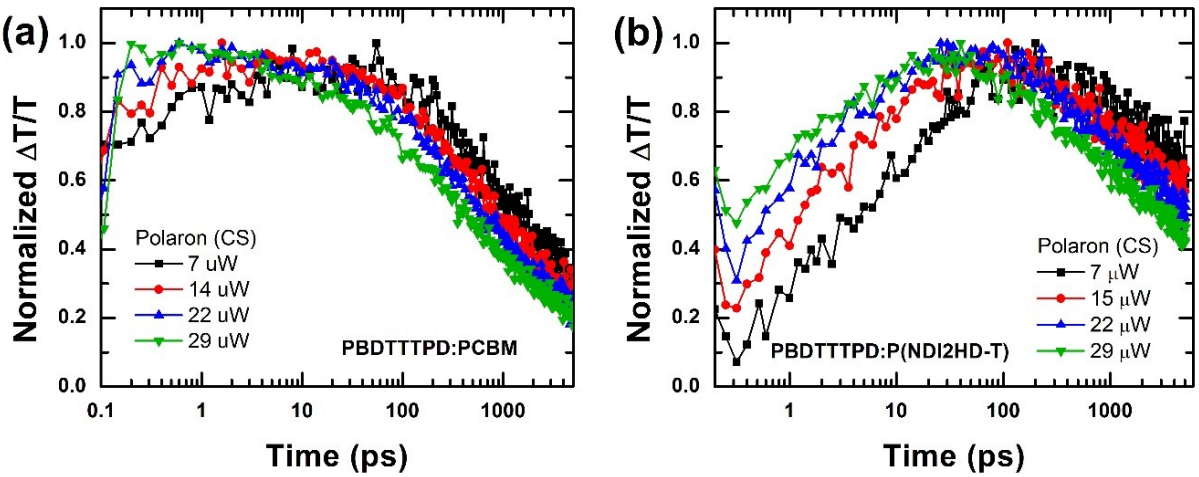

Figure S9. Fluence dependent dynamics of the CS peak before irradiation of the (a) PBDTTTPD:PCBM blended film and (b) PBDTTTPD:P(NDI2HD-T) blended film.

Table S4. Hole mobility (μ_h) and electron mobility (μ_e) values of the prisitine films with different illumination times.

Mobility	Material	0 h	6 h	12 h	24 h
μ_h (cm^2/V s)	PBDTTTPD only	3.33×10^{-5}	1.22×10^{-5}	2.66×10^{-5}	1.02×10^{-5}
μ_e (cm^2/V s)	PCBM Only	7.52×10^{-4}	5.35×10^{-5}	5.32×10^{-5}	5.14×10^{-5}
	P(NDI2HD-T) only	7.47×10^{-5}	8.34×10^{-5}	7.85×10^{-5}	7.48×10^{-5}

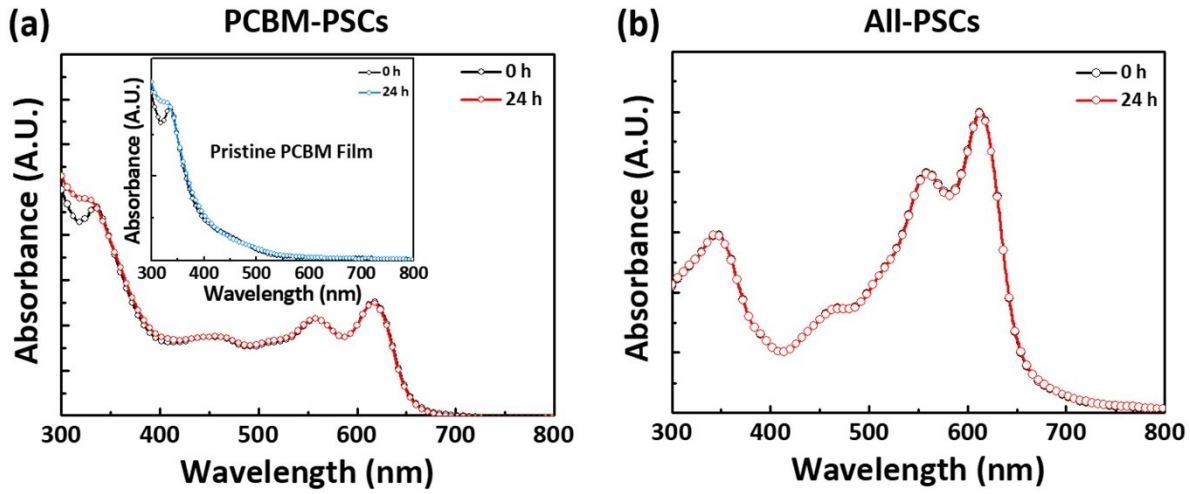

Figure S10. UV-vis absorption spectra of (a) PBDTTTPD:PCBM, (b) PBDTTTPD:P(NDI2HD-T) and pristine PCBM films (inset of **a**) before and after (24 h) illumination.

References

1. I. A. HOWARD, H. MANGOLD, F. ETZOLD, D. GEHRIG and F. LAQUAI, in *Ultrafast Dynamics in Molecules, Nanostructures and Interfaces*, WORLD SCIENTIFIC, 2014, DOI: 10.1142/9789814556927_0004, pp. 53-78.
2. F. Etzold, I. A. Howard, N. Forler, A. Melnyk, D. Andrienko, M. R. Hansen and F. Laquai, *Energy Environ. Sci.*, 2015, **8**, 1511-1522.
3. C. Dyer-Smith, I. A. Howard, C. Cabanetos, A. El Labban, P. M. Beaujuge and F. Laquai, *Adv. Energy Mater.*, 2015, **5**, 1401778.
4. T. Kim, J.-H. Kim, T. E. Kang, C. Lee, H. Kang, M. Shin, C. Wang, B. Ma, U. Jeong, T.-S. Kim and B. J. Kim, *Nat. Commun.*, 2015, **6**, 8547.